

Model based strategies for an optimised ribbing design of large forming tools

Nicholas Drude · Leopold Meier · Hartmut Hoffmann · Jürgen Scheurle

Received: 20 July 2009 / Accepted: 7 October 2009 / Published online: 29 October 2009
© German Academic Society for Production Engineering (WGP) 2009

Abstract A proposal is made for the ribbing of large forming tools. In the software developed for this purpose the ribbing structure is pre-optimised by means of an algorithm based on the power-law approach and then post-optimised with a newly developed algorithm for the reduction of the v. Mises stress. The model, intention and functioning of the software are explained. The optimised ribbing structures are analysed on parameterised test geometries and compared with conventional ribbing strategies in respect of manufacturing suitability, casting defects, mechanical properties and residual stress.

Keywords Topology optimisation · Casting · Forming tools · Simulation

1 Introduction

Large forming tools are constructed, on the side opposite to the active surface with ribbing to provide a sufficiently rigid geometry but with as low a tool weight as possible.

The ribbing is typically designed strictly according to internal company construction regulations with normally a rectangular or hexagonal layout of supports in the direction of the main strain [5, 9]. The ribbing design is not always tested by FE-simulation. In addition, homogeneous material properties are usually assumed as the manufacturing process is not taken into consideration. Forming tools are largely made of cast iron by the Lost Foam casting technique [2]. The casting design is determined based on the experience of the foundry and the constructing engineer. Up-to-date casting simulation programmes, by means of which mould filling, solidification, temperature distribution, residual stress, mechanical properties and casting defects can be calculated, are only applied in individual cases [7, 12], although their application is widespread in foundries.

Mathematical models for the ideal mechanical design layout are described under the concept of *topology optimisation* and have already been implemented in commercial simulation programmes. Among the approaches to topology optimisation the power-law approach described in [1] and [8] is predominant. An automatic consideration of the casting process regarding the inhomogeneity of material properties, the avoidance of casting defects, and the castability are generally not an issue in these optimisation algorithms [3–7, 10, 12]. The topology optimisation of forming tools is still at the planning and development stage in industry or it is only used to optimise individual aspects. In this paper new topologically optimised ribbing strategies are suggested, they are analysed in respect of mechanics, castability and manufacturing suitability and are compared with conventional ribbing strategies. Additionally, a possible way of achieving casting enhancement by the use of casting simulation data is described.

N. Drude · J. Scheurle
Technische Universität München, Zentrum Mathematik,
Lehrstuhl für Höhere Mathematik und Analytische Mechanik,
Garching, Germany
e-mail: drude@ma.tum.de

L. Meier (✉) · H. Hoffmann
Technische Universität München,
Lehrstuhl für Umformtechnik und Gießereiwesen,
Garching, Germany
e-mail: leopold.meier@utg.de

2 Mathematical model

2.1 Topology optimisation

The aim is to design a solid body \mathcal{B} (the forming tool) within an admissible domain $\Omega \subset \mathbb{R}^3$ (the design space) in such a way that the resulting *compliance* is minimal. Pre-defined loads and boundary conditions act upon \mathcal{B} , which is additionally subject to a volume upper limit. This optimisation task is named *minimum compliance problem*.

\mathcal{B} is characterised by its elasticity tensor field \mathbf{C} . The set of all admissible elasticity tensor fields is denoted by \mathcal{C} . The boundary $\partial\Omega$ of the design space Ω is the union of disjoint sets $\partial\Omega = \Gamma_1 \cup \Gamma_2 \cup \Gamma_3$, where $\Gamma_1, \Gamma_2 \neq \emptyset$. The forming tool \mathcal{B} is held along Γ_1 , and Γ_2 represents the active surface on which the load $\hat{\mathbf{s}}$ acts. The gravitational force is disregarded.

Let H^1 be the Sobolev space of displacement fields \mathbf{u} on Ω , which are supposed to be zero along Γ_1 , and $\epsilon(\mathbf{u})$ the linearised strain associated to \mathbf{u} . If the bilinear form $a(\mathbf{u}, \mathbf{v}) : H^1 \times H^1 \rightarrow \mathbb{R}$ and the functional $\ell : H^1 \rightarrow \mathbb{R}$ are defined by

$$a(\mathbf{u}, \mathbf{v}) := \int_{\mathcal{B}} \epsilon(\mathbf{u}) \cdot \mathbf{C}[\epsilon(\mathbf{v})] d\mathbf{v}$$

$$\langle \ell, \mathbf{v} \rangle := \int_{\Gamma_2} \hat{\mathbf{s}} \cdot \mathbf{v} da,$$

then the minimal compliance problem is

$$N.B. : \left. \begin{array}{l} \min \langle \ell, \mathbf{u} \rangle \\ a(\mathbf{u}, \mathbf{v}) = \langle \ell, \mathbf{v} \rangle, \quad \mathbf{v} \in H^1, \\ \mathbf{C} \in \mathcal{C}. \end{array} \right\} \quad (1)$$

In the power-law approach¹ \mathcal{C} is defined as the set of all elasticity tensor fields \mathbf{C} , such that

$$\left. \begin{array}{l} \mathbf{C}(\mathbf{x}) = \rho(\mathbf{x})^p \mathbf{C}_0(\mathbf{x}), \quad p > 1, \\ \int_{\Omega} \rho(\mathbf{x}) d\mathbf{x} \leq V, \\ 0 < \rho_{\min} \leq \rho(\mathbf{x}) \leq 1, \quad \mathbf{x} \in \Omega. \end{array} \right\} \quad (2)$$

\mathbf{C}_0 is the elasticity tensor of the underlying material GJS-700, which is assumed to be homogeneous and isotropic with the E-Modul $E = 165,5$ GPa and a Poisson ratio of $\nu = 0,27$. In (2), the design function ρ is an order parameter, which we view as a dimensionless relative density. V is the volume upper limit of \mathcal{B} . We set $p = 3$ and $\rho_{\min} = 10^{-3}$ for numerical reasons; $\rho_{\min} > 0$ ensures that the stiffness matrix cannot be numerically singular.

Finally, we have to determine \mathcal{B} from ρ_{*} , the optimal density calculated according to (2). For casting, we take \mathcal{B} to be a smoothed version of $1_{\{\rho_* \geq 1/2\}} \subset \Omega$. For further

usage in different software environments, the surface of \mathcal{B} has to be smooth.

2.2 Algorithm to reduce the v. Mises stress

In addition, an algorithm has been developed, which modifies an optimised ribbing geometry to reduce the thermally induced v. Mises stress [11], which is evaluated and imported by MAGMASOFT (see Sect. 3). Up to an arbitrary limit, mass can be added to the ribbing structure. Every surface-element of the ribbing structure is analysed for stress and strain. Density is added to and allocated around elements, which are judged as critical, in a steady, smooth and deterministic way. This heuristic procedure has the objective, that the cross sectional area under large stress is increased, which is supposed to reduce the residual stress. The computing time is less than a minute on a normal desktop PC.

3 Programming the optimisation software and gateways

Based on the mathematical model of the material distribution method presented in Sect. 2, a topological optimisation software has been programmed using the programming languages *C* and *Matlab* (The MathWorks, Inc., USA). The implementation is based upon the recommended programme code described in [8]. Programming gateways have been written between the optimisation software and Matlab as well as the casting simulation software *MAGMASOFT* (MAGMA GmbH, Aachen). In this way, the optimised geometry can be imported into the simulation software and the results of the simulation can likewise be read back into the algorithm described in Sect. 2.2. This allows to analyse and enhance a tool which has been optimised for stiffness, from a casting perspective.

4 Test geometries

To verify the mathematical model and to compare optimised geometries with conventional ribbing geometries through casting simulation and mechanical FE-analysis, a set of parameterised test geometries has been defined. The selection and definition of the parameters have been based on typical characteristics and dimensions of real tools. In order to allow a good experimental suitability and the verification of certain key predictions, the forming tool's active surface has been abstracted to a homogeneous top panel, and the bearing surfaces, bearing frames and side cavities have been omitted. For conventional ribbing, the

¹ Also SIMP model. For details cf. [1].

result is shown in Fig. 1a. The construction parameters for the variation of the ribbing are listed in Table 1.

Similarly, for the ribbing structure which is to be optimised the maximum space available is an area of 2m × 4m times a height described by the parameter H_x (Fig. 1a). The volume fraction of the total design space to be filled by material is determined by the parameter V_x . Notationally, the individual test geometries are characterised by combinations of those symbols.

Deep drawing forming tools are subjected to a wide range of load conditions depending on the part geometry. Thus, the force transmissions applied in the simulation model have been abstracted to three types. The standard homogeneous contact pressure (Fig. 1b) represents forming tools for spacious, flat parts (e.g. engine bonnets). The load generated by smaller parts with higher draw depths (e.g. gearboxes, B-pillars) is simulated by a contact pressure applied in the center of the active surface, either in a rectangular or a trapezoid area.

5 Optimised ribbing strategies

Vertical cross-sections of the optimised ribbing geometries have tree-like structures for all ribs (see Fig. 2). The rib diameter is the largest at the active surface. The narrowing of the rib is first superlinear and then retains an almost constant diameter up to the edge of the design frame. Outer ribs become narrower over a shorter distance than inner ones. Smaller ribs with the same structure are often placed in cavities.

Horizontal cross-sections have concentrically arranged ribs. Mass and wall thickness of a rib in relation to the other ribs have approximately a linear dependency on the

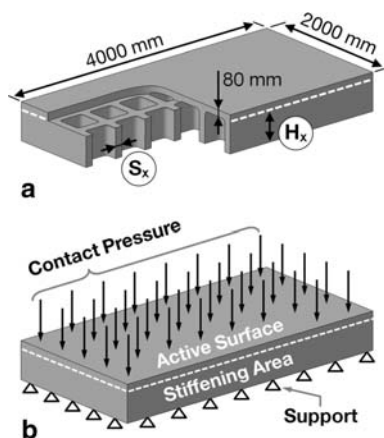


Fig. 1 a Construction parameters for the test geometries shown for a conventionally ribbed structure as an example; H_x = Ribbing height, S_x = Rib diameter; b boundary conditions and design space for topology optimisation

Table 1 Definition of the variable construction parameters of the test geometries

Variable	Description	Index (x)			Unit
		1	2	3	
H_x	Ribbing height	200	400	600	[mm]
V_x	Volume fraction	20	40	60	[%]
S_x	Rib diameter	40–160			[mm]

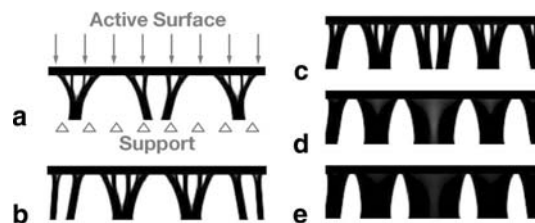


Fig. 2 Vertical sections of the design space in lateral direction (see Fig. 1b) showing the topologically optimised ribbing structure H_2V_x , $x \in \{1, 3/2, 2, 5/2, 3\}$; increasing ribbing proportion from a to e

force transmission acting on the rib. Given homogeneous force transmission, the distance between two ribs corresponds approximately to the wall thickness of the adjacent ribs. With inhomogeneous force transmission the distance between the ribs is approximately inversely proportional to the amount of force transmission.

The higher the design frame is, the fewer but stronger ribs turn out to be mechanically optimal. Generally speaking, for H_1 four ribs are optimal, for H_2 three and for H_3 two (see Fig. 3).

6 Comparison with conventional ribbing strategies

In the following evaluation of ribbing geometries, a colour-coded representation has been devised in which white represents a good result, grey a medium result and black represents a bad result.

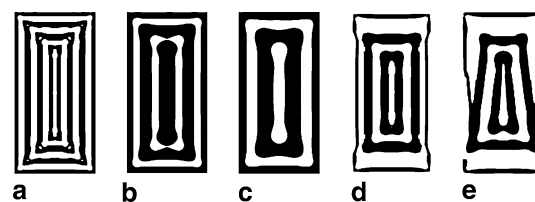


Fig. 3 Horizontal sections of the design space close to the support (see Fig. 1b) showing the topologically optimised ribbing structures; a H_1V_2 ; b H_2V_3 ; c H_3V_3 , all with homogeneous force transmission; d H_2V_2 with a stronger central force transmission; e H_2V_2 with a trapezoid central force transmission

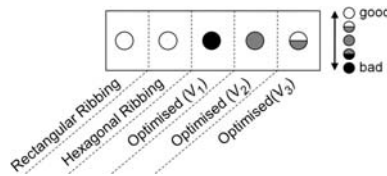


Fig. 4 Evaluation of manufacturing suitability with respect to the machining of the plastic foam model for lost foam casting

6.1 Manufacturing suitability

For the Lost Foam casting of large forming tools, a model is machined out of large plastic foam blocks. With multi-axial CNC machines, curved surfaces and slight undercuts can be made. Where larger undercuts are required, the plastic foam model must be manufactured in parts and glued together, which requires much more work and involves the risk of defects at the junctions of the parts. However, isolated cavities can only be produced by using supported sand cores which should be avoided if the process is to be economically acceptable. Conventional cross and hexagonal geometries predominantly contain flat surfaces and are therefore very well suited for the production of plastic foam models (Fig. 4).

The optimised geometries with low volume content (V_1) exhibit a tree-like branched structure with multiple isolated cavities and undercuts. They can only be cast with an excessive amount of effort. Optimised geometries with medium volume content (V_2) have a low number of cavities which can be virtually filled after optimisation to avoid the use of sand cores. Thus, the weight reduction in comparison to conventional ribbings is diminished. All in all, the V_2 geometries have a medium manufacturing suitability.

Optimised geometries with high volume content (V_3) are massively shaped and exhibit just slight undercuts. Their manufacturing suitability is generally good. However, due to the freeform surfaces, higher machining times are required compared to conventional geometries (Fig. 4).

6.2 Casting defects

Large forming tools normally contain a certain sum of shrinkage cavities and porosity, because the appropriate feeding technique to prevent these casting defects would be uneconomical. Nevertheless, porosity can only be tolerated, if it is located neither in sections with high working load induced stress nor close to surfaces which are to be machined. Thus, for the evaluation of the test geometries in respect to casting defects an evaluation scheme proposed by [5] has been used (Fig. 5).

In ribbing geometries with thin conventional ribs or a low volume optimised structure (V_1), the porosity is located close to the active surface. This is due to the low

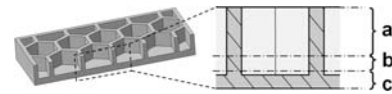


Fig. 5 Evaluation scheme for the influence of shrinkage cavities and porosity: **a** Noncritical section; **b** transition section; **c** critical section due to high load induced stress and possible damages to active surface, respectively

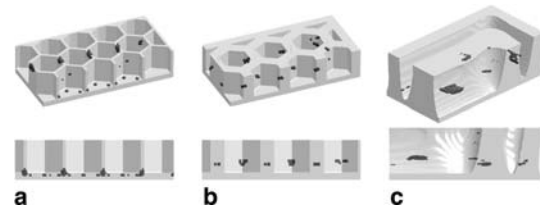


Fig. 6 Example of porosity probability in conventional and optimised ribbing geometries. Defect-free sections (porosity <1%) are displayed transparent **a**, **b** Hexagonal Ribbing with 40 mm and 160 mm rib diameter, resp., rib height H_2 ; **c** Optimised geometry H_3V_3

thermal mass of the ribbing, resulting in a minimum solidification rate at the junction between top plate and single ribs. These so called “hot spots” lead to volume defects like shrinkage cavities or porosity (Fig. 6a).

With increasing rib diameter and height, the position of the casting defects moves to uncritical sections (Figs. 6 and 7). Geometries with rectangular ribbing show slightly better results than hexagonal structures, since the connection of four ribs creates a bigger thermal mass resulting in a greater distance of the hot spots to the active surface. Given that ribbing height and volume are equivalent, the castability of the optimised geometries is comparable to conventional structures (Fig. 7).

However, high ribbing volume contents (V_3) can lead to open porosity at the rib flanks. The small amounts of moulding sand between the massive ribs heat up very fast, so that the hot spots are possibly located outside the rib (Fig. 6c).

6.3 Mechanical properties

The optimised geometries consistently show lower compliance than comparable conventional ribbings, mostly

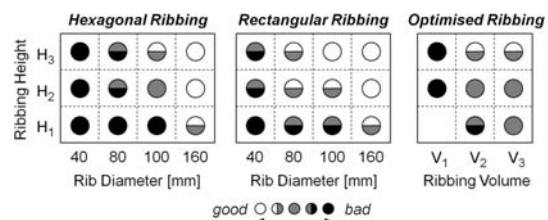


Fig. 7 Evaluation of the castability with respect to casting defects like shrinkage cavities and porosity

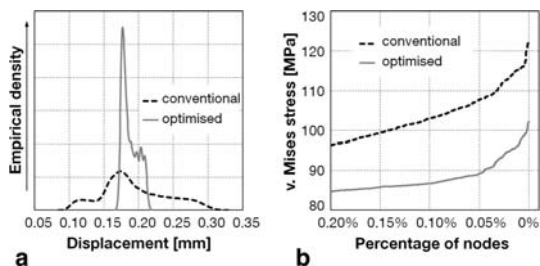


Fig. 8 **a** Analysis of the active surface deflection: empirical density estimate of the displacement of all FE-nodes of the active surface under loading vs. the displacement of these nodes; **b** extrem values: v. Mises stress vs. percentage of nodes at which the corresponding v. Mises stress is exceeded; in each case the test geometry H_2V_3 at a homogeneous active surface contact pressure of 30 MPa is analysed

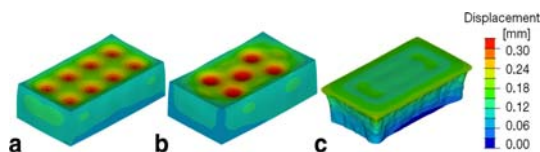


Fig. 9 Example analysis of the active surface deflection at a homogeneous contact pressure of 30 MPa: **a** Conventional rectangular and **(b)** hexagonal ribbing; **c** Optimised geometry H_2V_3 ; All structures have the same mass

between -5% and -15% . Furthermore, the distortion characteristics of the active surface is much better: The average variation from the medial surface deflection is 73% lower for the optimised geometries (Figs. 8a and 9).

For the deep-drawing process this uniform distortion yields the significant advantage, that a homogeneous pressure is applied to the blank between punch and forming die. This ensures a good and uniform material flow.

In addition, load induced stress peaks are consistently lower in optimised structures, on an average of -16% (Fig. 8b).

6.4 Residual stress

In respect to residual stress, the conventional ribbings are superior to the optimised. Their average residual stress is 26% lower, the stress peaks even 52% (Fig. 10).

The residual stress of all tested conventional geometries is below 160 MPa, which corresponds to the fatigue

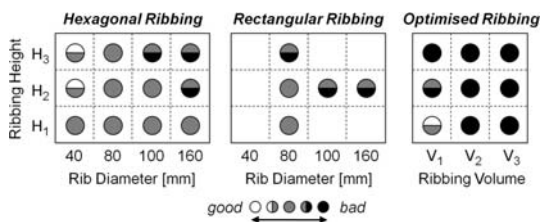


Fig. 10 Evaluation of the test geometries with respect to residual stress

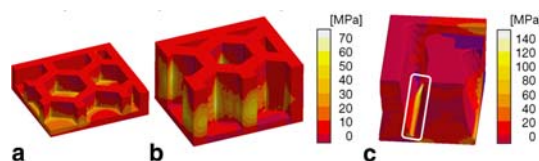


Fig. 11 **a, b** Example of residual stress simulations of conventional hexagonal ribbing geometries (maximum principal stress). The calculated stress level rises with increasing diameter and height of the ribs; **c** optimised geometry H_3V_3 with stress peaks in the rib base

strength of the analysed cast iron GJS-700 including a safety factor of 2. The maximum tensile stresses form at the rib junction edges. Generally, the stress level increases with higher rib diameters and heights (Figs. 10 and 11). Optimised structures show peaks of residual tensile stress in the rib bases (Fig. 11c), which increase with increasing ribbing volume (Fig. 10).

7 Consequences of the algorithm for the reduction of residual stress in casting

The algorithm reduces in every case the maximal v. Mises stress of the residual stress tensor, the extent depends, however, on whether the structure remains qualitatively identical by applying the algorithm or changes, e.g. two ribs are joined into one. If so, the maximal v. Mises stress is reduced by 32% on average, otherwise by 18%. The average v. Mises stress rises though, here the extent also depends on whether the structure changes qualitatively. If so, it rises on average by 39%, otherwise by 17%.

The sensitivity of casting parts to residual stress generally increases with increasing differences in the cross sectional area. In the test geometries, the highest residual stress peaks have been found at regions with small cross sectional areas like the rib bases and thin connection between the middle ribs (see Fig. 12). The mass distribution algorithm thickens up those critical regions, which reduces the cross-sectional area differences and thus the residual stress peaks. However, the reasons for the increase in the average stress level remain unclear.

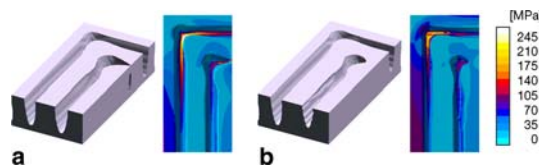


Fig. 12 Application of the algorithm for the reduction of residual stress on the test geometry H_2V_3 : **a** original geometry developed by the topology optimising software with high residual stress in the rib base; **b** geometry and residual stress after distribution of 5% of mass by the residual stress algorithm

8 Conclusion

In this work, the mathematical model and the newly developed software for the topology optimisation of large forming tool ribbings has been presented. Furthermore, optimised ribbing structures have been analysed and compared with conventional ribbing strategies on parameterised test geometries. The topology optimised ribbing geometries differ greatly from conventional ribbing structures. The standard design with rectangular or hexagonal layout of supports in the direction of the main strain yields the advantage of a good suitability for manufacture, parameterisation and standardisation. However, the castability with respect to porosity is limited. Topologically optimised structures allow to use the full material potential since they provide optimised mechanical properties like higher stiffness and extremely uniform distortions as well as considerable weight reductions. It must be pointed out, that these optimised structures are prone to high residual stress in the rib bases which compromise the load capacity. An empirical *rib base stress study* carried out separately shows that the residual stress formation depends on many geometrical parameters with complex interdependencies. A more detailed analysis of these influencing factors requires further research.

Acknowledgments The presented investigations have been carried out within the project “Mathematisch-gießtechnische Optimierung der Verrippung großer Umformwerkzeuge” funded by the German Research Foundation (DFG) under the contracts Ho 2165/28-1 and Sche 233/7-1.

References

1. Bendsøe M, Sigmund O (2004) Topology optimization. Springer, Berlin
2. Doege E, Behrens B (2007) Handbuch Umformtechnik. Springer, Berlin
3. du Maire E, Schmidt T (2005) Von der Natur lernen-kraftflussgerechte, neuartige Gestaltung gegossener Komponenten. Proceeding of the 2nd Newcast-Forum
4. Hessel C (2003) Integration der Topologieoptimierung in den CAD-gestützten Entwicklungsprozess. Diss RWTH Aachen, Shaker, Aachen
5. Hoffmann H et al (2007) Untersuchungen über optimale Rippenstrukturen von Umformwerkzeugen mit Hilfe der Gießsimulation. Konstr + giess 32(3):38–39
6. Katzenschwanz C, Friedrich M (2007) Angewandte Strukturoptimierung zur methodischen Leichtbaukonstruktion. Landshuter Leichtbau Colloquium
7. Schneider D (2008) Simulationsgestützte Untersuchung der Werkzeugbelastung beim Tiefziehen höchstfester Stähle. Diss TU München, Hieronymus, München
8. Sigmund O (2001) A 99 line topology optimization code written in Matlab. Struct Multidisc Optim 21:120–127
9. Siegert K, Häussermann M (2001) Weiterführende Untersuchungen zur Optimierung der Gestaltung von Umformwerkzeugen. EFB-Forschungsbericht Nr. 152, EFB e.V., Hannover
10. Trampert S, Beykirch R, Lauber B (2007) Vorsprung durch Strukturoptimierung bei der Motorenentwicklung. Automot Eng Partn, Special Issue 74
11. v Mises R (1913) Mechanik der festen Körper im plastisch-deformablen Zustand. Nachr Math Phys Göttingen 1913(4):582–592
12. v Schwerin ML (2008) Entwicklung einer Methodik zur optimierten Gestaltung von Umformwerkzeugen. Diss TU München, Hieronymus, München